Evaluating the capability of a critical state constitutive model to predict the collapse potential of loose sand

A. Azizi[1] **G. Bella**[2] **and I. Farshchi**[3]
[1]Polytechnic University of Milan, Milan, Italy
[2]Polytechnic University of Turin, Turin, Italy
[3]Linton University College, Negeri Sembilan, Malaysia

Many catastrophic flow failures in granular soil slopes are believed to be caused by a rise in pore water pressure associated with substantial loss of soil shear strength. This failure mechanism is known as prefailure instability or static liquefaction. Constant shear (CS) and consolidated undrained (CU) triaxial tests can reproduce stress paths, in which such instability may occur before reaching the failure. In the present study, a previously proposed critical state constitutive model was first used to simulate the behavior of loose saturated sand in CU tests. It was then employed to predict the instability of loose sand subjected to the CS loading. Under such loading, loose dry sand initially experience small volume increase, and then start to contract substantially. In saturated sand, such contractions can lead to the generation of pore water pressure and sudden decrease of shear strength. The capability of the model to predict the onset of the volume contraction and collapse potential of loose dry sand was examined by comparing the model predictions with experimental results of CS tests. The comparison showed that the effect of initial void ratio, consolidation and deviatoric stresses on behavior of loose dry sand can be well predicted by the model.

1. Introduction

Static liquefaction is known to be responsible for many disasters related to failures of geotechnical structures, such as flow failures of the submarine Nerlerk berm (Lade 1993) or north dike of Wachusett dam (Olsen et al. 2000). This failure mechanism is defined as the prefailure instability of the soil associated with a sudden loss of soil shear strength, resulting from an increase in pore pressure within the soil mass and a subsequent reduction in its effective stress. Consequently, flow failures initiated by static liquefaction leads to catastrophic damages as they rapidly develop with no noticeable warning.

The prediction of soil bahavior due to changes in stress state is a fundamental step in any geotechnical engineering project. Regarding to the widespread application of computational tools and important implication of instability in geotechnical engineering, the need for constitutive models capable of reproducing the soil behavior in stress paths, which leads to instability, is evident.

The present study provides a brief review on previous works concerning the instability of granular material, followed by introducing a previously proposed critical state constitutive model. The results of triaxial tests and relevant constitutive modeling are then represented. The model was first used to simulate the behavior of loose saturated sand in isotropic consolidated undrained (ICU) and constant

[1] Corresponding Author: Arash Azizi
Ph.D student, Polytechnic University of Milan, Milan, Italy
Piazza Leonardo da Vinci, 32, 20133 Milano
email: arash.azizi@polimi.it

shear (CS) tests. The capability of the model to predict the collapse potential of loose dry sand was then examined by comparing model predictions with experimental results of CS tests.

1.1 Instability of loose sand in experimental tests

Static liquefaction was first characterized as a sudden increase of pore water pressure and decrease of shear stress of loose saturated sand, induced by monotonic compression in undrained triaxial tests (e.g., Castro 1969, Sladen et al. 1985, Lade 1992, Yamamuro and Lade 1997, Leong et al. 2000, Wanatowski and Chu 2007). These studies illustrated that the deviatoric stress of a loose sand sample increases with little associated deformation, until the deviatoric stress is reached to the peak point before reaching the failure. Beyond the peak point, strain softening occurs as the pore pressure continues to increase. The Sample continues to deform until it reaches to the failure as shown in figure 1 (CU). Lade (1992) introduced the instability line (IL) passing through the peak points of undrained effective stress paths, in which the collapse of the granular material may occur above the stress ratio corresponding to the instability line. Figure 1 shows also the typical behavior of loose sand when the drainage is permitted. In consolidated drained (CD) compression triaxial test, the shear strength of the loose sample increases monotonically until it reaches the critical state strength, represented by the critical state line (CSL). It implies that the instability does not occur under monotonic compression loading as the drainage is permitted.

The prefilure instability can be triggered not only by an increase in external load, but also by a reduction in the effective mean stresses. An increase in pore water pressure resulting from infiltration of rainfall or snowmelt leads to a decrease in the mean effective normal stress, while the vertical load due to the weight of overlying soil does not change. It was observed that such a stress path can lead to the failure even under drained condition (e.g., Olsen et al. 2000). The CS triaxial test under drained condition, in which a constant deviatoric stress is applied to the top of a sample while the confining stress is decreased, reproduces a similar stress path. Numerous studies have been carried out to investigate the instability of both saturated and dry loose sand under the CS loading (e.g., Sasitharan et al. 1993, Skopek et al. 1994, Anderson and Riemer 1995, di Prisco and Imposimato 1997, Gajo et al., 2000, Chu et al. 2003, 2012, Daouadji et al. 2010). Previous studies have shown that cohesive, and medium to dense granular soils generally dilate when subjected to CS loading, while loose sand initially experience small or no volume change, and then start to contract substantially as failure is approached. If sand is saturated and drainage cannot occur fast enough, such contractions can lead to the generation of substantial pore water pressures and loss of strength. The same can happen in the field under drained condition, and the loss of soil strength may lead to the sudden, catastrophic failure of slopes. As shown in figure 1b, such instability takes place well above the instability line.

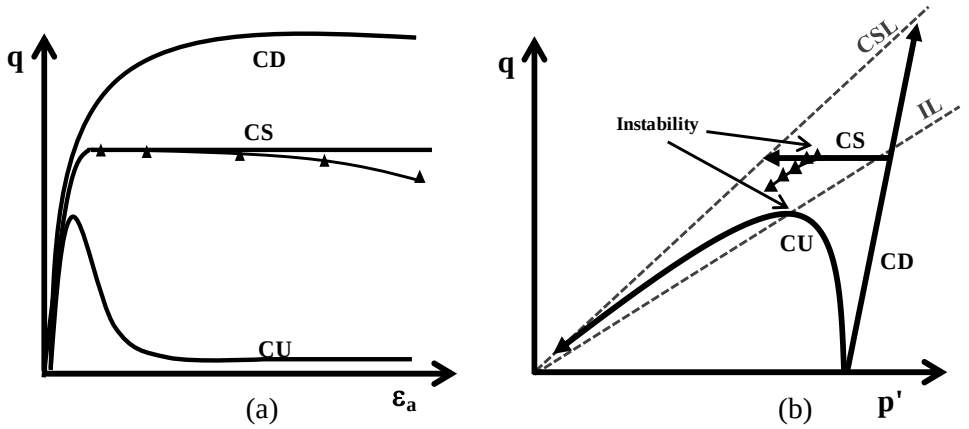

Figure 1. Typical behaviors of loose sand in triaxial consolidated drained (CD), consolidated undrained (CU) and constant shear (CS) tests: (a) the deviatoric stress-axial strain behaviors (b) the stress paths.

Beyond the instability, the saturated sample is unable to follow the prescribed stress path, experiencing loss of controllability (Nova 1994).

1.2 Critical state constitutive model (Imam et al. 2005)

The critical state constitutive model proposed by Imam et al. (2005) was adopted in this study. This model was developed with emphasis on taking into account important aspects of loose sand behavior. The constitutive relationships of the model are presented in the Appendix. This model consists of five elements: a capped yielding surface YS (equation [1]); a Mohr Coulomb failure criteria (equation [8]) which is a function of the friction angle and the current state parameter (Been and Jefferies, 1986); a flow rule based on Nova and Rowe's (1962) stress-dilatancy relationships combined with a modified form of equations used by Manzari and Dafalias (equation [9]); a hardening law (equation [10]); isotropic elasticity.

Figure 2a shows the capped yield surface (YS) of the model for different types of triaxial tests, namely, isotropic consolidated compression (IC), anisotropic consolidated extension (ACE) and anisotropic consolidated compression (ACC). The yield stresses and stress ratios are normalized to the mean normal stress at consolidation p_c. The Imam model is in fact a kinematic model, in which he yield surface changes its shape depending on the stress path.

Figure 2b shows the YS of isotropically consolidated sand with stress ratios at critical state (M_{CS}), at failure (M_f) and at peak deviatoric stress (M_P). The stress ratios M_P mentioned above control the shape of the yield surface, taking into account the effects of void ratio and mean normal stress, while the size of the yield surface is controlled by p_c. Figure 2b shows that in loose sand the stress ratio M_P is smaller than M_f. The peak stress ratio decreases with void ratio and confining pressure p_c and it takes values much smaller than M_{CS}.

The anisotropy is represented by another parameter, namely, α, in which the tangent of the yield surface is parallel to the q-axis. The parameter α is equal to zero in isotropic consolidation (IC), non-zero for anisotropic consolidation (AC). This parameter depends on the stress ratio at consolidation η_C, but it is assumed to be equal for compression and extension loading.

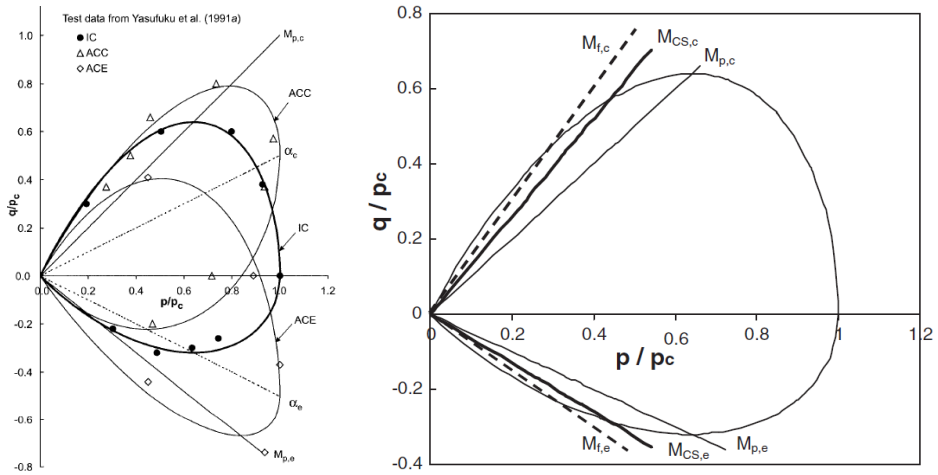

(a) (b)

Figure 2. (a) Yield surfaces for Yasufuku sand in isotropic consolidation (IC), anisotropic consolidation in compression (ACC) and anisotropic consolidation in extension (ACE) (b) Yield surface of isotropically consolidated sand with stress ratios corresponding to peak deviatoric stress, critical state and failure (Imam et al., 2005).

Table 1. Parameters of the model

Type	Parameter	Value
Peak state	φ_μ	24
	κ_p	1.2
Stress-dilatancy	φ_{cs}	33
	κ_{pT}	0.6
Plastic hardening	h	1
	C	0.024
Elasticity	G_r	5100
	K_r	17200
CSL	Γ	1.0121
	λ	0.0364

The model employs 10 parameters to simulate the sand behavior in triaxial compression loading over a wide range of void ratios and stresses. The parameters of the model used in this study are presented in table 1. These parameters were calibrated using the behavior of two loose samples in CU tests.

2. Material and sample preparation

All tests were carried out on a local uniform, subangular to angular, quartzic sand called the Firoozkooh No. 161 sand. The properties of the sand are listed in table 2. Samples were prepared using the moist-tamped technique, in which the samples with relatively 2 percent water content were gently tamped at 8 layers in order to obtain homogenous samples. The moist-tamped technique allows preparing samples with high void ratios. As reported by Ishihara (1993), the surface tension between soil grains generates a particular structure in soil samples prepared by the moist-tamped technique, so that upon undrained shearing there is a significant volumetric contraction. This is relevant to the aim of the present study.

Most CS tests were carried out on dry samples (or low moist samples as the water content of the samples was about 2 percent). However, a few CS and also all CU tests were carried out on saturated samples. For saturation, CO_2 was passed through the samples and followed by de-aired water percolation. Finally, the samples were assumed to be saturated if the B-Skempton value obtained at subsequent steps, in which the cell pressure and back pressure were increased simultaneously, was greater than 98 percent. For details, see Azizi et al. (2009).

Table 2. Properties of sand tested

Property	Firoozkooh No. 161
G_s	2.65
e_{max}	0.964
e_{min}	0.548
D_{50}	0.26
C_c	1.13
C_u	1.9
Angularity	Subangular to angular

3. Instability in Isotropic Consolidated Undrained Compression Test

Following saturation, the samples were consolidated isotropically to the effective stress desired for testing. Undrained tests were conducted under strain-controlled mode at a uniform strain rate of 1% per min, and the samples were sheared to large strain, mostly greater than 25%. As an undrained condition, samples were not allowed to drain during the shearing phase.

The results of ICU tests were used to obtain the critical state of the Firoozkooh sand. It is believed that for undrained behavior of any given sand, the shear strength at the critical state is only the function of void ratio. The slope of the CSL (M_{CS}) achieved by undrained tests was estimated to be about 1.28, which corresponds to the mobilized friction angle (ϕ_{CS}) of 33 degrees.

Figures 3a and 3c illustrate behavior of three samples in undrained monotonic compression loading. All samples were prepared at very low densities to ensure contractive responses and consolidated to the same confining pressures (250 kPa). The void ratios obtained at the end of consolidation (e_c) in tests CU87, CU96 and CU89 were 0.967, 0.922 and 0.903 respectively. Figure 3c shows that the ratio of q/p′ at the peak point of the effective stress path (M_P) decreases with an increase of void ratio. The experimental results showed that the stress ratio M_P changed not only due to void ratio variation, but also with changes of consolidation stress. M_P decreased as the state parameter at consolidation (ψ_c) increased. It implied that the slope of instability line of loose sand samples obtained from ICU tests decreased with an increase of void ratio and consolidation pressure.

Figures 3b and 3d show the model predictions for the behavior of the same samples. As illustrated the experimental results and the model predictions were consistent. The model was able to capture the effect of void ratio on the position of instability line in undrained isotropic compression tests. In fact, the model computes the stress ratio M_p which is a function of the state parameter (ψ) (equations 4 and 5), and employs M_p to control the shape of the yield surface.

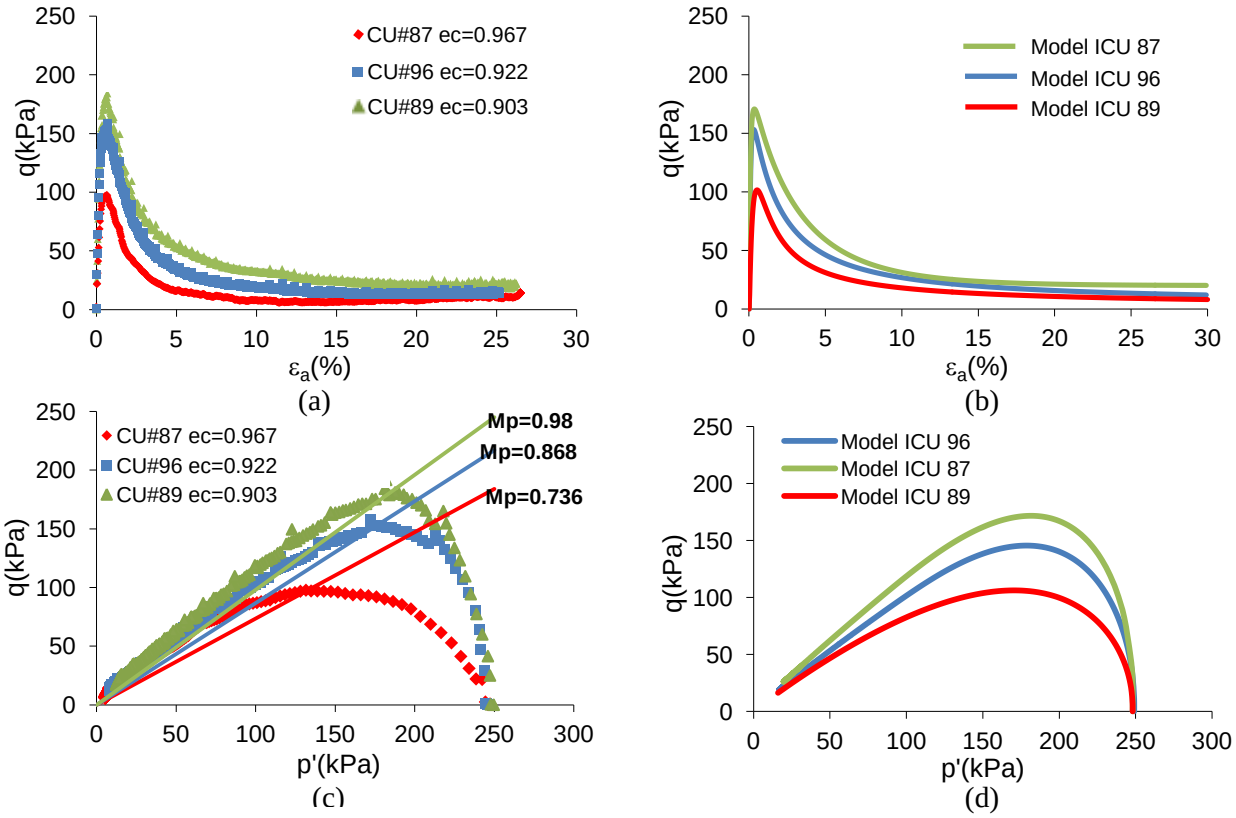

Figure 3. Undrained behavior of loose Firoozkooh sand samples and the model predictions.

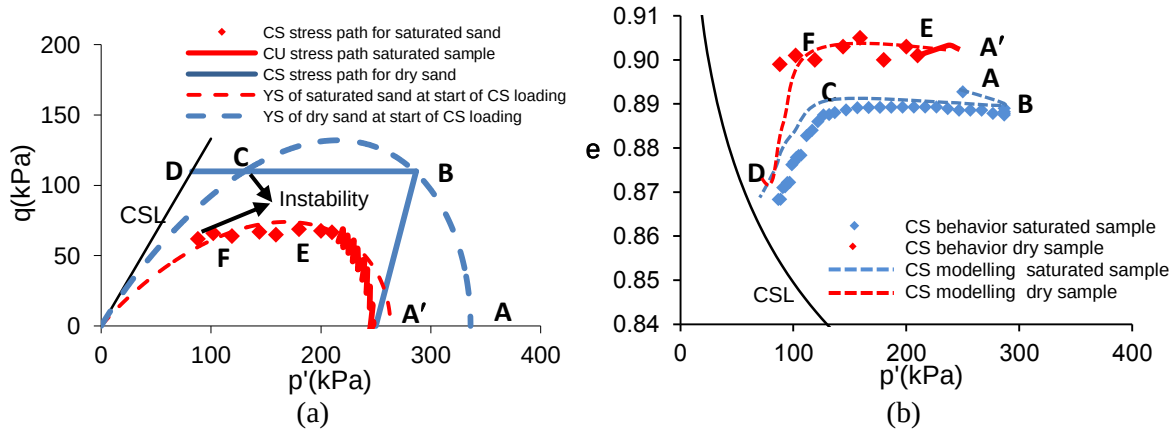

Figure 4. Behavior of dry and saturated loose sand in CDS loading and the model predictions (a) Stress paths (b) Void ratio changes.

4. Instability in Constant Shear Test

The stress path ABD in figure 4a represents CS loading, in which the dry sample was first isotropically consolidated to 250 kPa. The axial load was then increased (A-B) until the deviatoric stress reached to 110 kPa at point B. The deviatoric stress was then kept constant while the mean normal stress was reduced. The reduction in mean normal stress was continued until the soil state reaches the critical state in D. Figure 4b represents the variation of the void ratio for the same dry sample. Following the volume reduction caused by applying the axial load (A-B), the sample was slightly expanded while the cell pressure was decreasing (B-C). However, the sample started to contract substantially for further reduction in the cell pressure (point C). The same microstructural collapse of dry sand was observed by Skopek (1994).

Figure 4a shows also the yield surface of the dry sample established after applying the deviatoric stress and at the beginning of the CS loading. As pointed out by Imam et al. (2007), this yield surface passes through points B and C. In fact, the sample experiences unloading associated with a volume expansion while the CS loading is applied between B and C. As soon as the stress path reaches to the yield surface at point C, the instability occurs associated with volume contractions due to hardening of the yield surface, and it lasts until it reaches to CSL.

The CS test was also performed on saturated sample (stress path A′EF), in which the soil was first subjected to a conventional strain-controlled undrained triaxial compression loading until the desired deviatoric stress (63 kPa) was reached while mean effective stress was 217 kPa. Shearing was then stopped and the deviatoric load applied to the top of the sample was kept constant at the current state. The back pressure equal to the pore pressure at the end of undrained phase were applied to ensure no volume change of the sample would occur, and then second phase of the test began by gradually increasing the back pressure while drainage valve was opened and the cell pressure and deviatoric stress were kept constant. Therefore, the void ratio of the sample remained approximately unchanged from that achieved during isotropic consolidation (figure 4b). This resulted in the application of an almost constant deviatoric stress to the top of the sample, while the mean effective normal stress was being reduced under drained conditions. Approaching to the mean effective stress of 86 kPa at point F, saturated sample suddenly collapsed. The instability happened in such a rapid speed that it was impossible to record any data.

The mobilized friction angles at stress ratio where the collapse starts were similar for both saturated and dry samples. This mobilized friction angles were well below that of failure at the critical state (33 degrees). The friction angles reflect the stress states on YS that was established at the start of CS loading (point B for dry and point E for saturated sample), and this YS depends on both the current void ratio and the current stress state. Although the initial void ratio of the saturated sample (e=0.901) was greater compared to that of dry sample (e=0.882), but the hardening of the YS and decrease of the

stresses in undrained compression stress path resulted in state parameter and M_p similar to those of dry sample at the start of the CS loading. As a result, the saturated sample also experienced the elastic unloading within the stress path between E and F inside this YS until it approached to other side of the YS where the collapse occurred at point F.

5. Validating the capability of the model to predict the collapse of dry sand in CS tests

Although the sudden failure of saturated samples did not allow recording any data but it was possible to study the collapse behavior of dry samples. Thus, some CS tests carried on dry samples in order to examine the performance of the model considering the effect of different parameters on behavior of dry samples subjected to the CS loading.

5.1 Void ratio

Fig. 5 shows the results of CS tests on samples of Firoozkooh sand consolidated to 250 kPa and subjected to a constant deviatoric stress of 110 kPa. The void ratios obtained after consolidation (e_c) were different because the samples were prepared using different initial dry densities. The behaviors of these samples indicated that the samples experienced less volume contraction under CS loading as their void ratios obtained after consolidation (e_c) decreased. It may be noticed that the collapse potential for a dense material (e_c = 0.84) vanished and it experienced a continuous volume expansion. The onset of the volume contraction also occurred at smaller mean effective stresses and higher mobilized friction angles for samples with lower void ratios.

The effect of void ratios on the behavior of dry sand in the CS loading can be interpreted by the geometry of the YS established at the end of applying deviatoric stresse, i.e. at start of CS loading. The sample with higher void ratio had a higher state parameter, resulting in the yield surface with lower stress ratio M_p. As shown in figure 5a, the stress path approached to the YS at higher mean effective stress upon applying the CS loading for samples with higher void ratios. As a result, the distance between the onset of the collapse and the CSL, in which the volume contraction occurred, was greater. As the void ratio and state parameter of the samples decreased, M_p increased. Therefore, it established the YS with smaller distance between the onset of the collapse and the CSL leading to experience very small or no contraction during CS loading (samples with e_c=0.839).

The comparison between model predictions and experimental results showed that the model can predict the onset and severity of the collapse of dry samples in CS loading by taking into account the effect of the state parameter on the shape of the yield surface.

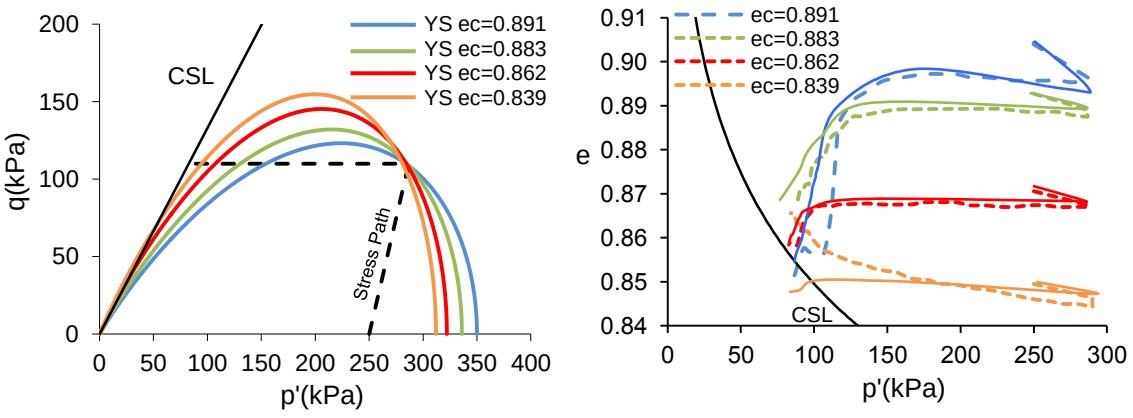

Figure 5. Effect of void ratio on sand behavior (dashed line) and model prediction (solid line) in the CS loading: (a) Stress paths (b) Void ratio changes.

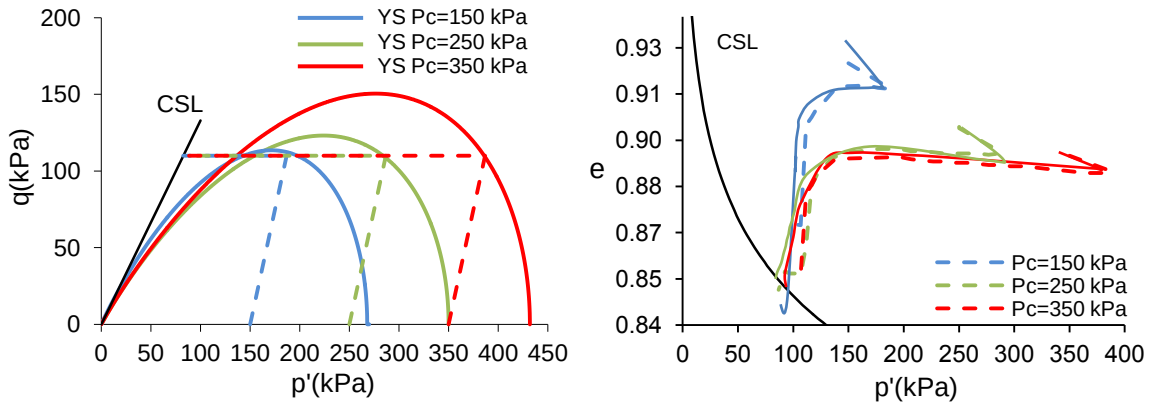

Figure 6. Effect of consolidation stress on sand experimental behavior (dashed line) and model prediction (solid line) in the CS loading: (a) Stress paths (b) Void ratio changes.

5.2 Confining pressure

The Samples were prepared using the same dry density and then consolidated to the mean normal stresses of 150, 250, and 350 kPa. Due to the different consolidation pressures, void ratios of the samples obtained after consolidation were not the same. Following the consolidation, all samples were subjected to the same deviatoric stress of 110 kPa.

The test results shown in figure 6 indicate that these samples had similar collapse potential as the volume contractions initiated at about the same mean normal stress and the amount of these volume contractions were approximately the same.

The state parameter controls the shape of the YS of this model. The samples with the higher confining pressures exhibited lower void ratio at the end of consolidation, and the higher confining pressure appeared to compensate for the decrease in void ratio. It implies that these samples had similar state parameters at the beginning of CS loading regardless of their confining pressures. It can be noticed from the YS of these samples (figure 6a) that they established yield surfaces with similar shapes but different sizes. The size of the elastic region developed at higher consolidation stress was larger, resulting in more unloading during the initial part of the CS loading. However, they reached to the similar mean normal stress where they met again their yield surfaces at the end of unloading. Consequently, they experienced the same amount volume contractions to reach to the CSL.

5.3 Deviatoric stress

The Samples were prepared at similar void ratio and consolidated to the same confining pressure of 250 kPa. They were then subjected to deviatoric stresses of 94, 110, 153, and 200 kPa, followed by the CS loading. The results of these tests shown in figure 7 indicated that in general, for samples subjected to higher deviatoric stress, as the confining pressure was decreased, the volume contractions were greater, and they started earlier.

Fig. 7a shows yield surfaces of the samples at the beginning of the CS loading. The state parameter, M_p and the shape of yield surfaces were the same for these samples. However, they established bigger yield surfaces as the applied deviatoric stress increased. It can be comprehended from the stress paths and the corresponding yield surfaces that the unloading distance during CS loading decreased for the samples with greater deviatoric stresses. The volume contractions commenced earlier and the collapse potential enlarged as the deviatoric stress applied before CS loading increased.

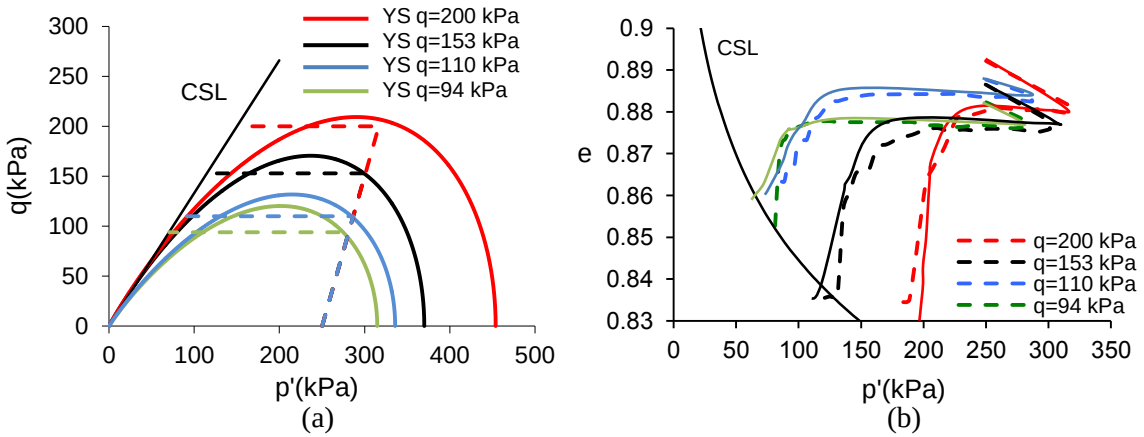

Figure 7. Effect of deviatoric stress on sand experimental behavior (dashed line) and model prediction (solid line) in the CS loading: (a) Stress paths (b) Void ratio changes.

6. Conclusion

The instability of loose saturated sand samples in undrained compression and constant shear tests was predicted by using the critical state constitutive model (Imam et al., 2005). The model employs the cap yield surface in which the shape of the yield surface is controlled by the instability line (stress ratio M_p), considering the effect of void ratio, mean normal stress and anisotropy. The instability and the behavior of loose sand in isotropic compression undrained tests were well predicted by the model.

The saturated loose sample subjected to the CS stress path exhibited a run-away failure due to the sudden increase of pore water pressure. The sample followed elastic unloading within the yield surface, established at the end of the undrained shearing, until it met the other side of the yield surface. The collapse occurred so fast that it was impossible to record any data.

The sudden increase of the pore water pressure in saturated sample was the consequence of the structural collapse and the volume contraction of dry samples in CS tests. In fact, the samples experienced unloading while the confining pressure was decreasing resulted in predicting elastic swelling by the model. It continued until the stress path reached the yield surface where it continued to show volume contraction as the yield surfaced hardened. The dry samples showed different collapse potential in tests performed at different initial void ratios, consolidation and deviatoric stresses. The onset of the collapse and the amount of volume contractions predicted by model were consistent with experimental results.

7. Appendix

The constitutive relationships of the model used in this study are summarized here. In general terms, the capped yield surface YS is defined as follow:

$$f = (\eta - \alpha)^2 - M_\alpha^2 \left[1 - \left(\frac{p}{p_c}\right)^{\frac{1}{2}}\right] = 0 \qquad [1]$$

where:

$$M_\alpha^2 = (5M_p - \alpha)(M_p - \alpha) = 0 \qquad [2]$$

p_c is the mean normal stress.

If the sand is isotropically consolidated (IC), $\alpha=0$ and [1] becomes:

$$\eta^2 - 5M_p^2 \left[1 - \left(\frac{p}{p_c}\right)^{\frac{1}{2}}\right] = 0 \qquad [3]$$

For triaxial compression TC, considering $\varphi_{p,c}$ as the friction angle at peak of undrained effective stress path in TC, the stress ratio $M_{p,c}$ is given by:

$$M_{p,c} = \frac{6sin\varphi_{p,c}}{3-sin\varphi_{p,c}} \quad [4]$$

whereφ_{μ} is the friction angle corresponding to zero state parameter ($\psi = 0$) in triaxial compression. The friction angles $\varphi_{p,c}$ is given by:

$$sin\varphi_{p,c} = sin\varphi_{\mu} - k_p\,\psi \quad [5]$$

where k_p is the model parameters, while ψ is the state parameter.
Considering φ_{cs} as the friction angle at the critical state and k_f as a constant parameter for sand in TC (k_f =0.75), the Mohr Coluomb failure criteria is defined using the following equation:

$$sin\varphi_f = sin\varphi_{cs} - k_f\,\psi \quad [6]$$

The failure friction angle φ_f obtained from [6] can be easily used to compute the maximum stress ratio $M_{f,c}$ according to [4] at the current soil state. Stress ratios can be different from the current stress ratio η, only at critical state $M_f = M_p = \eta$. The flow rule is the stress-dilatancy relationship proposed by Nova (1982) because of its simplicity for sands:

$$d = \frac{d\varepsilon_p^p}{d\varepsilon_p^q} = A(M_{cs} - \eta) \quad [7]$$

The rate of dilatancy is d, the volumetric plastic and deviatoric strains increments are $d\varepsilon_p^p$ ($d\varepsilon_p^p = d\varepsilon_1 + 2d\varepsilon_3$) and $d\varepsilon_p^q$ ($d\varepsilon_p^q = 2(d\varepsilon_1 - d\varepsilon_3)/3$) depending from the major ($d\varepsilon_1$) and minor ($d\varepsilon_3$) plastic strain increments. The term A is a material parameter (typically$A_c = 0.9$) for TC

$$A_c = \frac{9}{(9-2M_{pt,c}\eta+3M_{pt,c})} \quad [8]$$

It is worth to note that if A=1 eq. [7] became the same of Modified Cam Clay (Rocsoe et al. 1963), while stress ratios and $M_{pt,c}$ is given by:

$$sin\varphi_{pt,c} = sin\varphi_{cs} + k_{pt}\psi \text{ for TC} \quad [9]$$

The hardening law is expressed as follow:

$$\frac{\delta p_c}{d\varepsilon_q^p} = \frac{hG}{(p_f - p_c)_{ini}}\left(p_f - p_c\right) \quad [10]$$

where the mean normal stress at failure p_f is given by:

$$p_f = \frac{p}{\left[1-\frac{(M_f-\alpha)^2}{M_\alpha^2}\right]^2} \quad [11]$$

The term h is a non-dimensional material parameter depending to the sand stiffness during the shearing phase, G is the elastic shear modulus and $(p_f - p_c)_{ini}$ is the difference of $(p_f - p_c)$ after consolidation and before the shearing phase. Using G_r and K_r as reference values, elastic shear moduli G and elastic bulk moduli K are given respectively by:

$$G = G_r \frac{(2.973-e)^2}{1+e}\left(\frac{p}{p_a}\right)^{1/2} \quad [12]$$

$$K = K_r \frac{(2.973-e)^2}{1+e}\left(\frac{p}{p_a}\right)^{1/2} \quad [13]$$

Reference values are obtained from elastic moduli corresponding to the atmospheric pressure p_a.

NOTATION:

a_p, a_{PT}: Difference between $\sin\phi$ at peak point of the yield surface and at PT at ψ=0 in TC and TE, respectively
d: Soil dilatancy
e, e_{CS}: Current and critical state void ratios, respectively
f: Yield function
G, G_a: Elastic shear modulus at current and atmospheric mean normal stresses, respectively
h: Material parameter related to plastic shear stiffness
K, K_r: Elastic and reference bulk moduli, respectively
k_p, k_f, k_{PT}: Slope of variation of $\sin\phi_p$, $\sin\phi_f$ and $\sin\phi_{pt}$ with state parameter, respectively
M_{cs}, $M_{cs,c}$: Stress ratios q/p at critical state, and its values in TC, respectively
$M_p, M_{p,c}$: Stress ratio at the peak point of the yield surface, and its values in TC, respectively
M_μ, M_f: Stress ratio q/p corresponding to interparticle friction and failure, respectively
p, p_a, p_c, p_p, p_f: Efective mean normal stress, and its values at atmospheric pressure and at consolidation, respectively
q: Deviatoric stress
α: Stress ratio q/p at which tangent to yield surface is perpendicular to the p-axis
$\varepsilon_1, \varepsilon_3$: Major and minor principal strains respectively
$\varepsilon_p, \varepsilon_q, \varepsilon_p^p, \varepsilon_q^p$: Volumetric and shear strains and their plastic components, respectively
ϕ_f: Mobilized friction angle at failure
$\phi_{PT}, \phi_{PT,c}$: Friction angle at PT, and its values in TC, respectively
$\phi_p, \phi_{p,c}$: Friction angle at peak point of the yield surface, and its values inTC, respectively
ϕ_μ, ϕ_{cv}: Inter-particle and constant volume friction angles, respectively
η, η_c: Stress ratio q/p at current stress state and at consolidation, respectively
ψ: State parameter ($\psi = e - e_{cs}$)

8. References

[1] Anderson, S. A. and Riemer, M. F. 1995.Collapse of Saturated Soil Due to Reduction in Confinement. Journal of Geotechnical Engineering, ASCE, 121(2): 216–219.
[2] A. Azizi, R. Imam, A. Soroush, R. Zandian "Behavior of Sands in Constant Deviatoric Stress Loading", International Symposium on Prediction and Simulation Methods for Geohazard Mitigation (2009), Kyoto, Japan.
[3] Azizi, A. 2009. Experimental study and modelling of of sand behavior in constant deviatoric stress loading. MSc thesis, Amirkabir University of Technology.
[4] Been K. and Jefferies M.G., (1985). A state parameter for sands.Gèotechnique, Vol. 35, No. 2, pp. 99-112.
[5] Been K., Jefferies M.G., Hachley J.E., (1991). The critical state of sands.Gèotechnique, Vol. 41, No. 3, pp. 365-381.

[6] Castro G., (1969). Liquefaction of Sands.PhD thesis, Harvard Soil Mechanics Series 81, Harvard University, Cambridge, Massachusetts.
[7] Castro, G., Seed, R. B., Keller, T. O. and Seed, H. B. 1992. "Steady State strength analysis of the Lower San Fernando Dam Slide. Proc. of the 53rd Canadian Geotechnical Conference, Montreal, pp. 169–176.
[8] Chu, J., Lo, S-C. R., and Lee, I. K. (1993). "Instability of granular soils under strain path testing." J. Geotech. Eng., 119(5), 874–892.
[9] Chu, J., andWanatowski, D. (2009). "Effect of loading mode on strain softening and instability behavior of sand in plane-strain tests." J. Geotech. Geoenviron. Eng., 135(1), 108-120.
[10] Dafalias, Y., and Hermann, L.R. 1982. Bounding surface formulation of soil plasticity. In Soil mechanics-transient and cyclic loads. Edited by G.N. Pande and O.C. Zienkiewics. John Wiley & Sons, Chichester. Pp. 253-282.
[11] Daouadji, A., AlGali, H., Darve, F., and Zeghloul, A. (2010). "Instability of granular materials: Experimental evidence of diffuse mode of failure for loose sands." J. Eng. Mech., 136(5), 575-588.
[12] di Prisco, C., and Imposimato, S. (1997). "Experimental analysis and theoretical interpretation of triaxial load controlled loose sand specimen collapses." Mech. Cohes.-Frict. Mater, 2(2), 93-120.
[13] Eckersley, J. D. (1990). "Instrumented laboratory flowslides." Géotechnique, 40(3), 489-502.
[14] Gajo, A., Piffer, L., and de Polo, F. (2000). "Analysis of certain factors affecting the unstable behaviour of saturated loose sand." Mech. Cohes.-Frict. Mater, 5(3), 215-237.
[15] Imam, S. M. R., Morgenstern, N. R., Robertson, P. K., and Chan, D. H. 2005.A Critical State Constitutive Model for Liquefiable Sand. Canadian Geotechnical Journal, 42: 830–855.
[16] Imam, S. M. R., Morgenstern, N. R., Robertson, P. K., and Chan, D. H. 2002.Yielding and flow liquefaction of loose sand. Soils and Foundations, 42(3): 19-31.
[17] Imam, S. M. R., Morgenstern, N. R., 2007.Modeling sand Behavior in constant deviatoric stress loading. Soft Soil Engineering, pp. 389–395.
[18] Ishihara, K. 1993. Liquefaction and flow failure during earth-quakes. Geotechnique, 43(3): 351-415.
[19] Jefferies M.G., (1993). Nor-sand: a simple critical model for sand. Gèotechnique, Vol. 43, No. 1, pp. 91-103.
[20] Lade P.V., (1992). Static instability and liquefaction of loose fine sandy slopes. Journal of Geotechnical Engineering, Vol. 118, No. 1, pp. 51-71.
[21] Lade, P.V.: Initiation of static instability in the submarine Nerlerk berm, Canadian Geotechnical Journal, 30, 6, (1993) 895-904.
[22] Leong, W. K., Chu, J., and Teh, C. I. (2000). "Liquefaction and instability of a granular fill material." Geotech. Test. J., 23(2), 178–192.
[23] Olson, S.M., Stark, T.D., Walton, W.H., Castro, G.: 1907 Static liquefaction flow failure of the North Dike of Wachusett Dam, Journal of Geotechnical and Geoenvironmental Engineering, 126, 12, (2000) 1184-1193.
[24] Nova, R., 1982. Static A constitutive model for soil under monotonic and cyclic loading. In Soil mechanics-transient and cyclic loads. Edited by G.N. Pande and O.C. Zienkiewics. John Wiley & Sons, Chichester. Pp. 243-373.
[25] Nova, R. (1994). "Controllability of the incremental response of soil specimens subjected to arbitrary loading programs." J. Mech. Behav. Mater., 5(2), 193-201.
[26] Riemer, M. F. and Seed, R. B. Factors Affecting Apparent Position of Steady State Line. Journal of Geotechnical and Geoenvironmental Engineering,ASCE, 123(3): 281–287.
[27] Rowe, P.W. 1962.The stress-dilatancy relation for static equilibrium of an assembly of particles in contact. Pro.of the Roy.Soc.A269: 500–527.

[28] Sasitharan, S., Robertson, P. K., Sego, D. C. and Morgens-tern, N. R. 1994, Collapse behavior of sand, Canadian Geotechnical Journal, 30(4), pp.569-577.
[29] Skopek, P., Morgenstern, N. R., Robertson, P. K., and Sego, D. C. (1994). "Collapse of dry sand." Can. Geotech. J., 31(6), 1003-1008.
[30] Wanatowski, D., and Chu, J. (2007). "Static liquefaction of sand in planestrain." Can. Geotech. J., 44(3), 299–313.
[31] Yamamuro J.A. and Lade P.L., (1997). Static liquefaction of very loose sands.Canadian Geotechnical Journal, Vol. 34, pp. 905-917.